Modulations of SIR-nucleosome interactions of reconstructed yeast silent pre-heterochromatin by *O*-acetyl-ADP-ribose and magnesium

Shu-Yun Tung[a], Sue-Hong Wang[b], Sue-Ping Lee[a], Shu-Ping Tsai[a], Hsiao-Hsuian Shen[c], Feng-Jung Chen[c], Yu-Yi Wu[c], Sheng-Pin Hsiao[c], and Gunn-Guang Liou[a,c,d,*]

[a]Institute of Molecular Biology, Academia Sinica, Taipei 115, Taiwan; [b]Department of Biomedical Sciences, Chung Shan Medical University, Taichung 402, Taiwan; [c]Institute of Molecular and Genomic Medicine, National Health Research Institutes, Miaoli 350, Taiwan; [d]Guang EM Laboratory, New Taipei 242, Taiwan

ABSTRACT **Yeast silent heterochromatin provides an excellent model with which to study epigenetic inheritance. Previously we developed an in vitro assembly system to demonstrate the formation of filament structures with requirements that mirror yeast epigenetic gene silencing in vivo. However, the properties of these filaments were not investigated in detail. Here we show that the assembly system requires Sir2, Sir3, Sir4, nucleosomes, and *O*-acetyl-ADP-ribose. We also demonstrate that all Sir proteins and nucleosomes are components of these filaments to prove that they are SIR-nucleosome filaments. Furthermore, we show that the individual localization patterns of Sir proteins on the SIR-nucleosome filament reflect those patterns on telomeres in vivo. In addition, we reveal that magnesium exists in the SIR-nucleosome filament, with a role similar to that for chromatin condensation. These results suggest that a small number of proteins and molecules are sufficient to mediate the formation of a minimal yeast silent pre-heterochromatin in vitro.**

Monitoring Editor
Karsten Weis
ETH Zurich

Received: Jun 6, 2016
Revised: Nov 22, 2016
Accepted: Nov 29, 2016

INTRODUCTION

Nuclear DNA is packaged into chromatin with histones and other associated proteins and molecules. The nucleosome is the basic unit of chromatin organization. Approximately 146 base pairs of DNA are wrapped twice around an octamer core of histones (H2A, H2B, H3, and H4), comprising the first-level chromatin structure of a ~10-nm bead-on-a-string nucleosomal array. Magnesium and linker histone (H1) are essential for higher-order chromatin structure condensation into ~30-nm chromatin fibers (Sen and Crothers, 1986; Makarov *et al.*, 1987; d'Erme *et al.*, 2001; Strick *et al.*, 2001; Alberts *et al.*, 2002; Dorigo *et al.*, 2004; Huynh *et al.*, 2005).

Epigenetics is a DNA sequence–independent inheritance phenomenon of chromatin (Jenuwein and Allis, 2001; Moazed, 2001; Richards and Elgin, 2002). Epigenetic processes encompass modifications and modulations of DNA, histones, and other chromatin-associated proteins and molecules, thereby influencing chromatin structure to modulate DNA repair, recombination, replication, and gene expression. Epigenetic modification of histones modulates their affinity for DNA and for histone-associated proteins (Jenuwein and Allis, 2001; Moazed, 2001; Richards and Elgin, 2002). Therefore epigenetic modifications of histones can contribute to the dynamic changes between silent heterochromatin and active euchromatin.

The silent heterochromatin of budding yeast, *Saccharomyces cerevisiae*, serves as a good model system for studying epigenetic inheritance. The silent information regulator (Sir) proteins Sir2, Sir3, and Sir4 are required to create silent heterochromatin domains at the telomeres and the mating-type loci (Klar *et al.*, 1979; Rine and Herskowitz, 1987; Gottschling *et al.*, 1990; Aparicio *et al.*, 1991; Grunstein and Gasser, 2013; Kueng *et al.*, 2013; Oppikofer *et al.*, 2013). Sir proteins form the SIR complex, which binds to the nucleosome for the assembly of silent heterochromatin (Moretti *et al.*, 1994; Moazed and Johnson, 1996; Moazed *et al.*, 1997;

This article was published online ahead of print in MBoC in Press (http://www.molbiolcell.org/cgi/doi/10.1091/mbc.E16-06-0359) on December 8, 2016.

*Address correspondence to: Gunn-Guang Liou (bogun@gate.sinica.edu.tw; emguang@yahoo.com.tw).

Abbreviations used: AAR, *O*-acetyl-ADP-ribose; Ac, acetylation; AMP, monophosphate; EDS, energy dispersive spectrum; EM, electron microscopy; H, histidine residue; K, lysine residue; MALDI-TOF, matrix-assisted laser desorption ionization time-of-flight; Me, methylation; me3, trimethylation; Sir, silent information regulator; TXRF, total reflection X-ray fluorescence; Y, tyrosine residue.

Strahl-Bolsinger *et al.*, 1997). Sir2 is a NAD-dependent histone deacetylase (Imai *et al.*, 2000; Landry *et al.*, 2000) that couples deacetylation with NAD hydrolysis and synthesizes a metabolic small molecule, *O*-acetyl-ADP-ribose (OAADPR, or simply AAR; Tanner *et al.*, 2000; Sauve *et al.*, 2001; Tanny and Moazed, 2001). Sir3 and Sir4 preferentially bind to the hypoacetylation of histone H3 and H4, which requires the enzymatic activity of Sir2 (Tanny and Moazed, 2001; Hoppe *et al.*, 2002). Furthermore, Sir2 and Sir3 bind to the telomeric and mating-type regions, which also requires Sir2 enzymatic activity (Tanny *et al.*, 1999; Hoppe *et al.*, 2002; Luo *et al.*, 2002; Rusche *et al.*, 2002).

Purified Sir2 and Sir4 are present as a heterodimer containing varying amounts of Sir3 (Hoppe *et al.*, 2002; Rudner *et al.*, 2005). Purified Sir3 exists as dimer and higher-order oligomers (Liou *et al.*, 2005). Deacetylation of histones and generation of AAR promote the association of multiple copies of Sir3 with Sir2/Sir4 and induce a dramatic structural rearrangement of the SIR complex (Liou *et al.*, 2005). Therefore deacetylation and AAR may be a requirement of and contribute to SIR complex assembly and silent heterochromatin formation, although it has been reported that both Sir2 and AAR can be bypassed in transcriptional silencing (Yang and Kirchmaier, 2006; Chou *et al.*, 2008).

AAR is generated by Sir2 family proteins from bacteria, yeast, and human, but its exact biological role and even its interaction partner(s) in the nucleus are not yet fully known. Hst2, a yeast Sir2 homologue, can cocrystallize with AAR and a histone peptide (Zhao *et al.*, 2003). Similarly, macroH2A1.1 (mH2A1), a histone variant, has been identified as a binding partner of ADP-ribose and AAR (Kustatscher *et al.*, 2005). Furthermore, it has been reported that Sir2 associates with AAR (Tung *et al.*, 2012).

Based on the spreading of SIR complexes along the chromatin fiber, a model of silent heterochromatin formation has been proposed (Hoppe *et al.*, 2002; Luo *et al.*, 2002; Rusche *et al.*, 2002). An in vitro assembly system for filament structures has been developed using purified Sir proteins, yeast nucleosomes, and NAD (Onishi *et al.*, 2007). Although these filaments display requirements that closely mirror those observed in the formation of silent heterochromatin in vivo, the mechanisms and regulation of heterochromatin formation and even the detailed properties of in vitro–mimicking filament structures remain to be investigated.

In this study, we used molecular biological and biophysical methods, together with bioinformatics, to analyze the features of in vitro–assembled filament structures in an optimized assembly system. Using limited purified native proteins and molecules, we reconstructed a minimal yeast silent pre-heterochromatin that was modulated by AAR and magnesium.

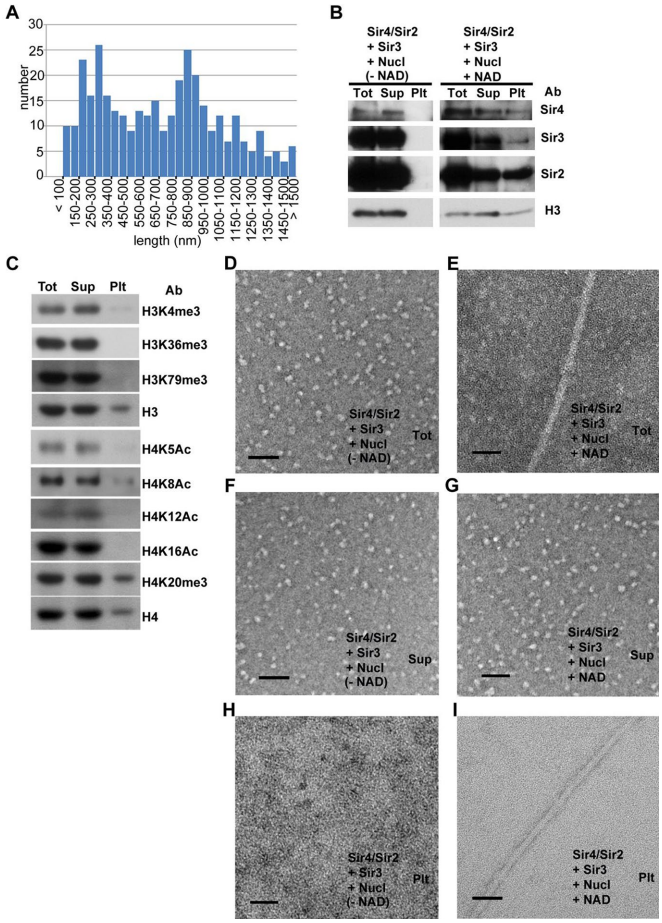

FIGURE 1: Validation of SIR-nucleosome filaments. (A) Histogram showing the bimodal distribution of the lengths of SIR-nucleosome filaments. The sample data were randomly recorded from two grids for each in vitro assembly reaction and three replicates. (B) Western blots of the pellet (Plt) and supernatant fractions (Sup) after ultracentrifugation of the in vitro assembly reaction (Tot) containing Sir4/Sir2, Sir3, and nucleosomes and with NAD absent (left) or present (right), detected by Sir4, Sir3, Sir2, and histone H3 antibodies, respectively, as indicated. (C) Western blot of the Plt and Sup after ultracentrifugation of Tot, detected by the various histone modification antibodies as indicated. (D–H) Electron micrographs showing the negatively stained Tot, Sup, and Plt portions of in vitro assembly reactions containing Sir4/Sir2, Sir3, and nucleosomes with NAD absent (D, F, H) or present (E, G, I). Electron micrographs were randomly selected from two grids for each sample with three replicates. Bar, 100 nm.

RESULTS AND DISCUSSION

Validation of in vitro–assembled SIR-nucleosome filaments

In a previous study, we developed a filamentous structure assembly system in vitro using purified Sir proteins, nucleosomes, and NAD (Onishi *et al.*, 2007). The features of this filament were not well characterized, however, and the optimal reaction conditions also remained to be established.

First, we conducted analyses to verify the properties of these assembled filamentous structures. Under electron microscopy (EM), the filaments were clearly observed and easily distinguished from the ball-shaped structure of the nucleosome and Sir proteins. For each examination of the assembly reaction, we used at least two grids and at least three replicates. Typically, one to six filaments were observed within half the aperture of a 200-mesh grid. Overall the filaments were 15–20 nm (18.1 ± 1.9 nm) in diameter and >100 nm in length (Figure 1, A and E, and Supplemental Figure S1E). This meant that the filaments were too large and too long to represent those expected for any one of the Sir proteins, single SIR complexes, or single nucleosomal dimers or tetramers (Supplemental Figure S1, B–E). Furthermore, the lengths of filaments exhibited a bimodal distribution (712 ± 377 nm; maximum, 1962 nm; minimum, 123 nm; median, 701 nm; first mode of group, 300–350 nm; second mode of group, 850–900 nm; 354 samples; Figure 1A). These varying lengths implied that end-to-end joining of oligonucleosome fragments occurred in the assembly reaction. AAR-stabilizing Sir3 interactions probably contributed to this finding (unpublished data). However, the detailed mechanism of how this process could cause an extended longer filament remains to be investigated. In our assembly system, we noted

that only some proteins were assembled into filaments (45 ± 2, 18 ± 2, 33 ± 5, and 20 ± 1% for Sir2, Sir3, Sir4, and H3, respectively; Figure 1B), possibly because our purified native nucleosomes contained various histone modifications that represent dynamically different chromatin states, such as euchromatin, heterochromatin, or chromatin under transcription/translation or replication. However, only the enzymatic substrates of Sir2 (i.e., the acetylation of histone lysine residues, such as H4K16Ac and H4K12Ac, but not other modifications of histone, such as H3K79Me and H4K20Me) should have been able to associate with Sir2 to initialize the first step of filament assembly. In the assembled filaments, acetylations of histone 4 lysine 12 and lysine 16 (H4K12Ac & H4K16Ac) and trimethylations of histone 3, lysine 36, and lysine 79 (H3K36me3 and H3K79me3) could not be detected. In contrast, trimethylation of histone 4 and lysine 20 (H4K20me3) was detected. However, a weak signal was detected by H4K8Ac antibody, and very minor signals of H4K5Ac and H3K4me3 were traceable in the assembled filaments (Figure 1C). These filaments may represent a yeast heterochromatin-like structure mimic in vivo. In addition, when any one of the Sir proteins, nucleosomes, or NAD was absent in our in vitro assembly system, no filaments were detected (Supplemental Figure S1, F–I). These results indicate that all of these components are necessary for in vitro filament assembly and that the filaments might be SIR-nucleosome filaments. Because the filaments were not as wide as traditional 30-nm heterochromatin, they might represent an intermediate condensation state of heterochromatin and might continue to interact with other proteins/molecules to further condense, so we call them SIR-nucleosome pre-heterochromatin filaments.

To determine the presence of Sir proteins and nucleosomes in the filaments using electron microscopy, we ultracentrifuged the assembly reactions at speeds sufficient to pellet down the filaments but not the individual reaction components. Aliquots of the resuspended pellet and supernatant portions were analyzed by Western blot and checked by electron microscopy (Figure 1, B, E, G, and I). Sir2, Sir3, Sir4, and histone H3 were all detected in the pellet portion when the filament assembly conditions included the presence of NAD (Figure 1B, right) in the standard assembly system (Figure 1C). However, when NAD was absent from the assembly reaction, filamentous structures did not form (Figure 1, D, F, and H), as described previously. Under the same ultracentrifugation conditions, Sir2, Sir3, Sir4, and histone H3 could not be detected in the putative pellet portion (Figure 1B, left). Thus all Sir proteins and histone H3 protein contributed to the formation of these filamentous structures, and the assembled filaments can be considered SIR-nucleosome filaments.

Modulation of SIR-nucleosome filament assembly by AAR

Because AAR is known to play an important role in regulating SIR complex assembly (Liou *et al.*, 2005), we were interested to determine whether AAR also plays a distinct role in the mechanism of our SIR-nucleosome filament formation. We used an enzymatically inactive Sir2 mutant, Sir2-H364Y (Figure 2A and Supplemental Figure S2A), to address this issue. The mutation does not affect the ability of the protein to assemble into the SIR complex or the regulation of SIR complex assembly by AAR (Liou *et al.*, 2005). We used adenosine monophosphate (AMP) as another structure-based relative metabolic small molecule as a control. AAR can be degraded to AMP by the Ysa1 protein (Lee *et al.*, 2008), and AMP is recognized as an intermediate metabolite of AAR.

In contrast to SIR-nucleosome filaments containing wild-type Sir2 (Figure 1C), no long filamentous structure formed in the assembly reactions containing Sir2-H364Y in the presence of NAD (Figure 2B). This suggests that the enzymatic activity of Sir2 was

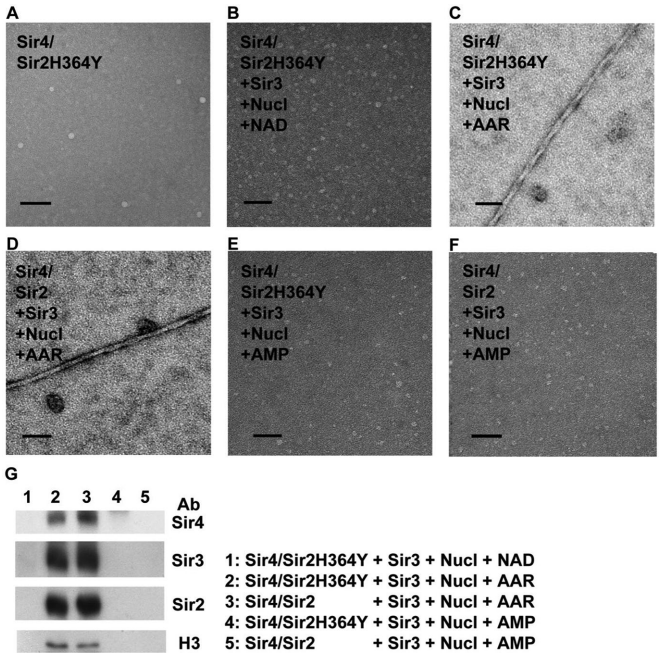

FIGURE 2: Modulation of SIR-nucleosome filament formation by AAR. (A) Electron micrograph showing the negatively stained purified Sir4/Sir2H364Y. (B, C) Electron micrographs showing the in vitro assembly reactions containing Sir4/Sir2H364Y, Sir3, and nucleosomes in the presence of NAD (B) or AAR (C). (D) Electron micrograph showing the in vitro assembly reaction containing Sir4/Sir2, Sir3, and nucleosomes in the presence of AAR. (E, F) Electron micrographs showing the in vitro assembly reactions containing either Sir4/Sir2 (E) or Sir4/Sir2H364Y (F) with Sir3, nucleosomes, and AMP. (G) Western blot of the pellet fractions after ultracentrifugation of in vitro assembly reactions, detected by Sir4, Sir3, Sir2, and histone H3 antibodies, respectively, as indicated. Reaction components in each lane are listed on the right. Electron micrographs were randomly selected from two grids for each sample with three replicates. Bar, 100 nm.

responsible for the formation of the SIR-nucleosome filaments in the assembly reactions. Next we wanted to determine whether AAR—a native enzymatic metabolite of Sir2—could regulate the formation of SIR-nucleosome filaments. As shown in Figure 2C, purified AAR (Supplemental Figure S2B) promoted the formation of SIR-nucleosome filaments in our assembly reaction containing Sir2-H364Y. The same result was also observed in assembly reactions containing wild-type Sir2 in the presence of AAR but not in the absence of NAD (Figure 2D). After ultracentrifugation as described in the previous section, Sir4, Sir3, Sir2, and histone H3 were detected in the resuspended pellet portions of these filamentous structures by Western blot assays (Figure 2G). In addition, no filamentous structure was observed in assembly reactions containing the AMP control under both wild-type and mutant Sir2 conditions (Figure 2, E and F). Further, Sir4, Sir3, Sir2, and histone H3 were not detected in the putative pellet portions of these AMP control reactions by Western blot assays (Figure 2G). We conclude that the epigenetic metabolic small molecule AAR acts as a modulator to regulate the formation of SIR-nucleosome filaments.

The distributions of SIR proteins on SIR-nucleosome pre-heterochromatin filaments in vitro and on telomeres in vivo

With the use of EM and immunogold-labeled antibodies specific to each of the Sir proteins, each of the Sir protein types could be

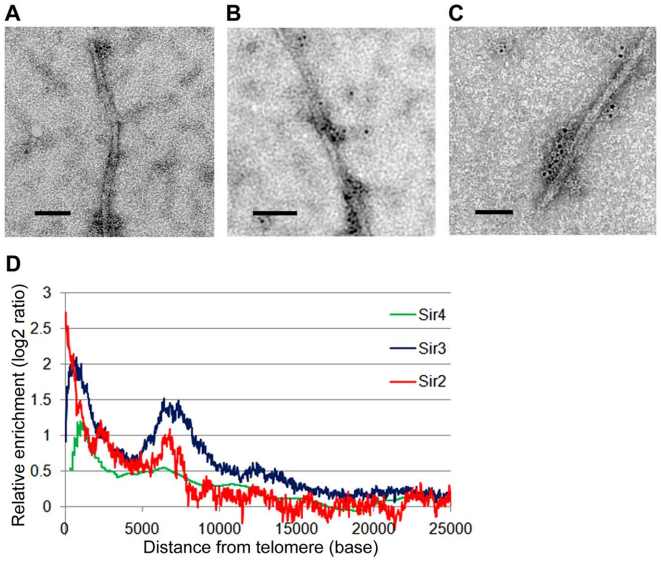

FIGURE 3: Distribution patterns of Sir proteins. (A–C) Electron micrographs showing the in vitro–assembled SIR-nucleosome filaments immunogold-labeled by Sir2 (A), Sir3 (B), and Sir4 (C) antibodies. (D) The moving averages of Sir2, Sir3, and Sir4 binding at all 32 yeast telomeres plotted as a function of distance from the chromosome ends. Binding enrichment was measured as the log 2 score of immunoprecipitation vs. input. Electron micrographs were randomly selected from two grids for each experiment with at least three replicates. Bar, 100 nm.

detected on the filaments and displayed interesting and discontinuous localization patterns (Figure 3, A–C). The major localization of Sir2 was at the terminal region of the filaments, whereas Sir3 was never detected in this region, and Sir4 was rarely localized there. The extent of distribution of Sir3 on filaments was similar to that of Sir4 but was greater than that of Sir2. In addition, the two discontinuous regions of Sir2 localization were more widely separated than the discontinuous regions of Sir3 localization and those of Sir4. We failed to detect immunogold signal for histone H3 or histone H4 antibodies on the filaments. This could be because the recognized epitopes were covered due to tight packaging of the nucleosomes, which are entirely surrounded by associated Sir proteins, thereby concealing the recognized epitopes on the outer surface of the filaments. We noticed that some filaments showed a helical shape (Figures 1, C and E, and 2, C and D) and that both the Sir3 and Sir4 signals seemed to show a helical distribution (Figure 3, B and C). Whether these characteristics arise because Sir proteins tend to surround the nucleosomes helically or because of a feature of the filament itself remains to be investigated. Although purified Sir2/Sir4 and Sir3 are able to individually associate with histone proteins without NAD or AAR present, AAR is able to induce stoichiometric change and structural rearrangement of SIR complexes. Sir3 shows a higher affinity toward Sir2/Sir4 and histones after self-polymerization (Liou *et al.*, 2005). The results suggest that an individual Sir3 oligomer interacts with nucleosomes along some parts of the SIR-nucleosome filament in the absence of Sir2. However, we cannot rule out the possibility that Sir4 may also associate with nucleosomes in these regions lacking Sir2 due to either structural rearrangement of SIR complexes or Sir3 interaction with Sir4 (Liou *et al.*, 2005) or to the possibility of individual Sir4s interacting with nucleosomes.

Using available data bank information (National Center for Biotechnology Information Gene Expression Omnibus: GSE3360, GSE65672) and the concept that SIR complexes binding to the telomere indicates the presence of silent heterochromatin, we plotted Sir2, Sir3, and Sir4 enrichment as a moving average function of distance from the telomeres (Sperling and Grunstein, 2009; Tung *et al.*, 2013) to examine the distribution profiles of Sir2, Sir3, and Sir4 on telomeres. As expected, distributions of Sir2, Sir3, and Sir4 on the telomeric DNA regions for all chromosomes generally roughly overlapped (Figure 3D). Of interest, however, we found that the highest relative enrichment ratio of Sir2 on telomeres was at the termini, with signal decreasing thereafter, but with other signal peaks at around positions 2.5 and 6.5 kb. In contrast, the signals of highest relative enrichment ratio for Sir3 and Sir4 were not at the terminus but at around position 1.5 kb, with another broader signal peak at around position 6.5–7.5 kb. Thus the distribution pattern of Sir2 was not the same as for those of Sir3 and Sir4. In conclusion, these distribution patterns on telomeres in vivo agreed with the immunogold-labeling signal patterns on SIR-nucleosome pre-heterochromatin filaments in vitro.

SIR-nucleosome pre-heterochromatin filaments contain magnesium

We found that magnesium was required for pre-heterochromatin formation when modifying our assembly system to determine optimum reaction conditions. When the reaction buffer contained various cations such as calcium or zinc instead of magnesium, the assembled filaments were ~10–15 nm (13.6 ± 2.1 and 12.7 ± 2.1 nm, respectively) in diameter and were thinner than the typical 15- to 20-nm (18.1 ± 1.9 nm) filaments assembled in the reaction buffer system containing magnesium (Figure 4, A–D). The difference in the average values between the two groups (Mg vs. Ca, and Mg vs. Zn) was greater than would be expected by chance. That is, there was a statistically significant difference ($p < 0.001$). In contrast, the difference in the average values for Ca versus Zn was not sufficient to exclude the possibility that the difference was due to random variability. Hence there was not a statistically significant difference ($p = 0.125$; Figure 4D). This finding suggests that magnesium functions in our system in a way similar to the well-known magnesium-dependent chromatin condensation.

It is possible that magnesium not only affects assembly processing, but also exists in the pre-heterochromatin filaments. We used energy dispersive spectrum (EDS) analysis of EM to explore this possibility. According to EDS, the spectral peaks of SIR-nucleosome pre-heterochromatin filaments revealed that the in vitro–assembled pre-heterochromatin contained magnesium (Figure 4E). We noted that the magnesium signal was weaker than the major carbon (supporting film on the grid) and copper (material of the grid) signals. However, this signal was more pronounced than background signals of the buffer control or signals of various reaction conditions (such as using zinc instead of magnesium; Figure 4F). Moreover, the magnesium signal was present only in the pre-heterochromatin filaments and not in the individual reaction protein components, such as Sir2/4, Sir3, and nucleosomes. A zinc signal was not detected in the thinner filaments when zinc replaced magnesium in the reaction buffer (Figure 4F). In addition, total reflection x-ray fluorescence (TXRF) analysis revealed a significant magnesium signal in the SIR-nucleosome pre-heterochromatin filaments (Figure 4G). Together these results indicate that magnesium was chelated by the pre-heterochromatin filaments during their formation and is also required for pre-heterochromatin condensation. However, where and how the magnesium is chelated by protein(s) or DNA alone or cooperatively require further study.

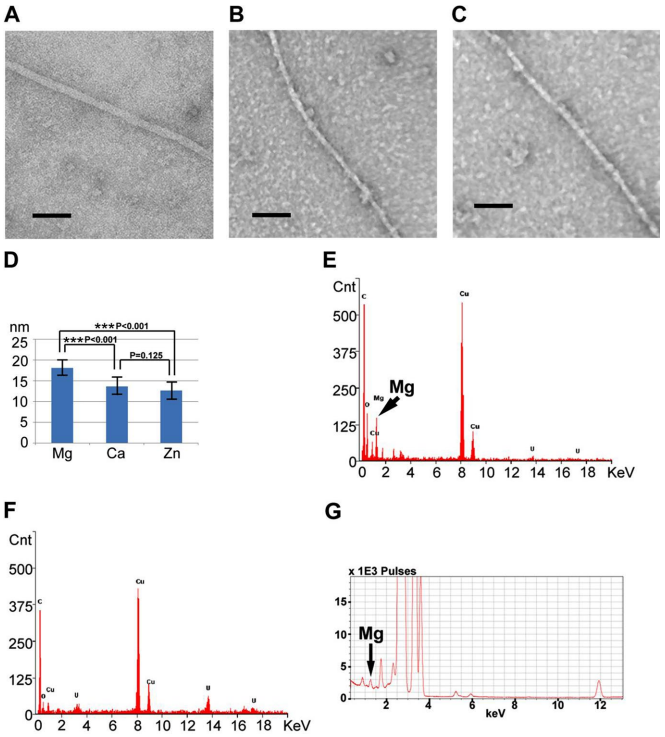

FIGURE 4: Magnesium on SIR-nucleosome filaments. (A–C) Electron micrographs showing the in vitro assembly reactions containing Sir4/Sir2, Sir3, nucleosomes, and NAD in the presence of buffer containing magnesium (A), calcium (B), or zinc (C). Electron micrographs were randomly selected from two grids for each experiment with three replicates. Bar, 100 nm. (D) Histogram showing the differences in diameters of SIR-nucleosome filaments in reaction buffers containing magnesium, calcium, or zinc, as indicated. (E, F) EDS analysis of EM results used to examine in vitro–assembled SIR-nucleosome filaments in reaction buffers containing magnesium (E) or zinc (F). (G) TXRF analysis was used to further examine in vitro–assembled SIR-nucleosome filaments, in which a clear magnesium signal was detected.

Recently a reconstruction of condensed mitotic chromatids using minimal components in vitro was reported (Shintomi *et al.*, 2015). However, the condensed structure and the cellular function of mitotic chromatids may be different to those of silent heterochromatin. Condensed mitotic chromatids are involved in chromosome segregation during cell division and should be more densely packaged. Silent heterochromatin involves dynamic changes from active euchromatin during DNA repair, recombination, replication, and gene expression. Therefore the heterochromatin structure could be less condensed to more easily and efficiently process chromosome remodeling.

In conclusion, our reconstructed minimal yeast silent SIR-nucleosome pre-heterochromatin should be a good candidate material for further research in the fields of molecular biology, epigenetics, and small molecules.

MATERIALS AND METHODS

Purification of proteins and AAR

Methods for the purification of Sir3, Sir4/Sir2, Sir4/Sir2H364Y, native yeast nucleosomes, and AAR were based on previously described methods (Liou *et al.*, 2005; Onishi *et al.*, 2007; Tung *et al.*, 2012). Protein samples were separated on SDS–PAGE and then stained by silver nitrate or Coomassie brilliant blue R520 to visualize protein bands. Purified AAR was verified by matrix-assisted laser desorption ionization time-of-flight mass spectrometry.

Assembly of SIR-nucleosome pre-heterochromatin

In vitro assembly reactions were based on previously described methods (Onishi *et al.*, 2007; Tung *et al.*, 2012) with optimized modifications. Purified Sir3 (~0.8 mg/ml), nucleosomes (~0.2 nM), and either wild-type Sir4/Sir2 (~0.5 mg/ml) or mutant Sir4/Sir2H364Y (~0.5 mg/ml) were incubated with or without NAD (~10 mM), AMP (~8 mM), or AAR (~8 mM) (as prescribed by the indicated experimental design reaction conditions) in a reaction buffer (50 mM 4-(2-hydroxyethyl)-1-piperazineethanesulfonic acid–KCl, pH 7.6, 300 mM KCl, 4 mM $MgCl_2$/$CaCl_2$/$ZnCl_2$) of a 10-ml reaction volume. These mixtures were incubated at room temperature for 2–4 h or overnight with rocking at 4°C.

Ultracentrifugation of in vitro assembly reactions

Samples of various in vitro assembly reactions were subjected to ultracentrifugation at 100,000 × *g* for 30 min in a TLA-100 rotor using a Beckman Optima TL-100 ultracentrifuge. The supernatants and pellets were recovered, resolved by SDS–PAGE, and analyzed by Western blot with individual antibodies as indicated.

Assays of electron microscopy

Samples prepared for EM analysis were examined as previously described (Liou *et al.*, 2001; Onishi *et al.*, 2007; Chen *et al.*, 2013) with some modifications. For negative-staining, 3-µl samples were individually absorbed onto a glow-discharged, 200-mesh copper grid covered with a carbon-coated collodion film, washed with three drops of distilled water, and stained with two drops of 0.75% uranyl formate. The samples were examined using an FEI Tecnai T12, a Hitachi H7650, a Jeol 1400, or a Jeol 2100F electron microscope. For immunogold labeling, 15-µl samples were individually absorbed onto a glow-discharged, 200-mesh nickel grid covered with a carbon-coated collodion film. The grids were then floated on 5% normal goat serum in phosphate-buffered saline (PBS) for 15 min and floated on the individual primary antibodies as indicated for 15–30 min. After six sequential washings with 20-µl droplets of 1% normal goat serum in PBS, the grids were floated for 15–30 min on the 10 nm gold–immunoglobulin G complexes. Grids were then washed sequentially with six droplets of 1% normal goat serum in PBS, followed by two 3-min washes with triple-distilled water. Grids were finally treated with two drops of 0.75% uranyl formate and examined by EM as for the negatively stained samples. For EDS analysis, the sample preparation procedure was the same as that used for negative-staining, and the elemental analyses were conducted using a Hitachi H7650 or a Jeol 1400 electron microscope equipped with an EDS detector.

Total reflection x-ray fluorescence analysis

TXRF analysis was conducted on a S2 PICOFOX instrument. Briefly, 10 µl of sample was spotted on the quartz slide, dried on a heating plate, and set onto the polished carrier disk to detect the signals by an XFlash detector.

ACKNOWLEDGMENTS

We thank Danesh Moazed, Thomas Walz, Megumi Onishi, and Sue Lin-Chao for helpful discussions and resource support and Hsilin Cheng, Wen-Li Peng, Yu-Ching Chen, Yi-Yun Chen, I-Hui Chen, Paul Wei-Che Hsu, Eason Yeh, and the members of G.-G.L.'s lab for

technical help and Alex Wang at Bruker for helping with TXRF analysis. Chung-Shi Yang at the National Health Research Institutes, Yeu-Kuang Hwu at the Academia Sinica and National Synchrotron Radiation Research Center, and Wei-Hau Chang at the Academia Sinica kindly provided access to a Hitachi-H7650 EM, a Jeol 2100 EM, and a Jeol 1400 EM, respectively. The Institute of Molecular Biology, Academia Sinica, kindly provided access to an FEI Tecnai G2 spirit EM to generate the results. This work was supported by Ministry of Science and Technology, Taiwan R.O.C. (grants NSC 102-2311-B-400-002 and MOST 103-2311-B-400-002), and National Health Research Institutes, Taiwan R.O.C. (grant MG 103-PP-08).

REFERENCES

Alberts B, Johnson A, Lewis J, Raff M, Roberts K, Walter P (2002). Chromosomal DNA and its packaging in the chromatin fiber. In: Molecular Biology of the Cell, 4th ed., New York: Garland Science, 198–216.

Aparicio OM, Billington BL, Gottschling DE (1991). Modifiers of position effect are shared between telomeric and silent mating-type loci in *S. cerevisiae*. Cell 66, 1279–1287.

Chen F-J, Lee K-W, Lai C-C, Lee S-P, Shen H-H, Tsai S-P, Liu B-H, Wang L-M, Liou G-G (2013). Structure of native oligomeric Sprouty2 by electron microscopy and its property of electroconductivity. Biochem Biophys Res Commun 439, 351–356.

Chou CC, Li YC, Gartenberg MR (2008). Bypassing Sir2 and O-acetyl-ADP-ribose in transcriptional silencing. Mol Cell 31, 650–659.

d'Erme M, Yang G, Sheagly E, Palitti F, Bustamante C (2001). Effect of poly(ADP-ribosyl)ation and Mg2+ ions on chromatin structure revealed by scanning force microscopy. Biochemistry 40, 10947–10955.

Dorigo B, Schalch T, Kulangara A, Duda S, Schroeder RR, Richmond TJ (2004). Nucleosome arrays reveal the two-start organization of the chromatin fiber. Science 306, 1571–1573.

Gottschling DE, Aparicio OM, Billington BL, Zakian VA (1990). Position effect at *S. cerevisiae* telomeres: reversible repression of Pol II transcription. Cell 63, 751–762.

Grunstein M, Gasser SM (2013). Epigenetics in *Saccharomyces cerevisiae*. Cold Spring Harb Perspect Biol 5, a017491.

Hoppe GJ, Tanny JC, Rudner AD, Gerber SA, Danaie S, Gygi SP, Moazed D (2002). Steps in assembly of silent chromatin in yeast: sir3-independent binding of a Sir2/Sir4 complex to silencers and role for sir2-dependent deacetylation. Mol Cell Biol 22, 4167–4180.

Huynh VAT, Robinson PJJ, Rhodes D (2005). A method for the in vitro reconstitution of a defined "30 nm" chromatin fiber containing stoichiometric amounts of the linker histone. J Mol Biol 345, 957–968.

Imai S, Armstrong CM, Kaeberlein M, Guarente L (2000). Transcriptional silencing and longevity protein Sir2 is an NAD-dependent histone deacetylase. Nature 403, 795–800.

Jenuwein T, Allis CD (2001). Translating the histone code. Science 293, 1074–1080.

Klar AJS, Fogel S, MacLeod K (1979). MAR1-a regulator of the HMa and HMalpha loci in *Saccharomyces cerevisiae*. Genetics 93, 37–50.

Kueng S, Oppikofer M, Gasser SM (2013). SIR proteins and the silent chromatin in budding yeast. Annu Rev Genet 47, 275–306.

Kustatscher GI, Kustatscher G, Buhecha HR, Allen MD, Pugieux C, Sait F, Bycroft M, Ladurner AG (2005). The macro domain is an ADP-ribose binding module. EMBO J 24, 1911–1920.

Landry J, Sutton A, Tafrov ST, Heller RC, Stebbins J, Pillus L, Sternglanz R (2000). The silencing protein SIR2 and its homologues are NAD-dependent protein deacetylases. Proc Natl Acad Sci USA 97, 5807–5811.

Lee S, Tong L, Denu JM (2008). Quantification of endogenous sirtuin metabolite O-acetyl-ADP-ribose. Anal Biochem 383, 174–179.

Liou G-G, Jane W-N, Cohen SN, Lin N-S, Lin-Chao S (2001). RNA degradosomes exist in vivo in *Escherichia coli* as multicomponent complexes associated with the cytoplasmic membrane via the N-terminal region of ribonuclease E. Proc Natl Acad Sci USA 98, 63–68.

Liou G-G, Tanny JC, Kruger RG, Walz T, Moazed D (2005). Assembly of the SIR complex and its regulation by O-acetyl-ADP-ribose, a product of NAD-dependent histone deacetylation. Cell 121, 515–527.

Luo K, Vega-Palas MA, Grunstein M (2002). Rap1-Sir4 binding independent of other Sir, yKu, or histone interactions initiates the assembly of telomeric heterochromatin in yeast. Genes Dev 16, 1528–1539.

Makarov VL, Smirnov I, Dimitrov SI (1987). Higher order folding of chromatin is induced in different ways by monovalent and by bivalent cations. FEBS Lett 212, 263–266.

Moazed D (2001). Common themes in mechanisms of gene silencing. Mol Cell 8, 489–498.

Moazed D, Johnson D (1996). A deubiquitinating enzyme interacts with SIR4 and regulates silencing in *S. cerevisiae*. Cell 86, 667–677.

Moazed D, Kistler A, Axelrod A, Rine J, Johnson AD (1997). Silent information regulator protein complexes in *Saccharomyces cerevisiae*: a SIR2/SIR4 complex and evidence for a regulatory domain in SIR4 that inhibits its interaction with SIR3. Proc Natl Acad Sci USA 94, 2186–2191.

Moretti P, Freeman K, Coodly L, Shore D (1994). Evidence that a complex of SIR proteins interacts with the silencer and telomere-binding protein RAP1. Genes Dev 8, 2257–2269.

Onishi M, Liou G-G, Buchberger JR, Walz T, Moazed D (2007). Role of the conserved Sir3-BAH domain in nucleosome binding and silent chromatin assembly. Mol Cell 28, 1015–1028.

Oppikofer M, Kueng S, Gasser SM (2013). SIR-nucleosome interactions: structure-function relationships in yeast silent chromatin. Gene 527, 10–25.

Richards EJ, Elgin SC (2002). Epigenetic codes for heterochromatin formation and silencing: rounding up the usual suspects. Cell 108, 489–500.

Rine J, Herskowitz I (1987). Four genes responsible for a position effect on expression from HML and HMR in *Saccharomyces cerevisiae*. Genetics 116, 9–22.

Rudner AD, Hall BE, Ellenberger T, Moazed D (2005). A nonhistone protein-protein interaction required for assembly of the SIR complex and silent chromatin. Mol Cell Biol 25, 4514–4528.

Rusche LN, Kirchmaier AL, Rine J (2002). Ordered nucleation and spreading of silenced chromatin in *Saccharomyces cerevisiae*. Mol Biol Cell 13, 2207–2222.

Sauve AA, Celic I, Avalos J, Deng H, Boeke JD, Schramm VL (2001). Chemistry of gene silencing: the mechanism of NAD+-dependent deacetylation reactions. Biochemistry 40, 15456–15463.

Sen D, Crothers DM (1986). Condensation of chromatin: role of multivalent cations. Biochemistry 25, 1495–1503.

Shintomi K, Takahashi TS, Hirano T (2015). Reconstitution of mitotic chromatids with a minimum set of purified factors. Nat Cell Biol 17, 1014–1023.

Sperling AS, Grunstein M (2009). Histone H3 N-terminus regulates higher order structure of yeast heterochromatin. Proc Natl Acad Sci 106, 13153–13159.

Strahl-Bolsinger S, Hecht A, Luo K, Grunstein M (1997). SIR2 and SIR4 interactions differ in core and extended telomeric heterochromatin in yeast. Genes Dev 11, 83–93.

Strick R, Strissel PL, Gavrilov K, Levi-Setti R (2001). Cation-chromatin binding as shown by ion microscopy is essential for the structural integrity of chromosomes. J Cell Biol 155, 899–910.

Tanner KG, Landry J, Sternglanz R, Denu JM (2000). Silent information regulator 2 family of NAD-dependent histone/protein deacetylases generates a unique product, 1-O-acetyl-ADP-ribose. Proc Natl Acad Sci USA 97, 14178–14182.

Tanny JC, Dowd GJ, Huang J, Hilz H, Moazed D (1999). An enzymatic activity in the yeast Sir2 protein that is essential for gene silencing. Cell 99, 735–745.

Tanny JC, Moazed D (2001). Coupling of histone deacetylation to NAD breakdown by the yeast silencing protein Sir2: evidence for acetyl transfer from substrate to an NAD breakdown product. Proc Natl Acad Sci USA 98, 415–420.

Tung S-Y, Hong J-Y, Walz T, Moazed D, Liou G-G (2012). Chromatin affinity-precipitation using a small metabolic molecule: its application to analysis of O-acetyl-ADP-ribose. Cell Mol Life Sci 69, 641–650.

Tung S-Y, Lee K-W, Hong J-Y, Lee S-P, Shen H-H, Liou G-G (2013). Changes in the genome-wide localization pattern of Sir3 in *Saccharomyces cerevisiae* during different growth stages. Comput Struct Biotechnol J 7, e201304001.

Yang B, Kirchmaier AL (2006). Bypassing the catalytic activity of SIR2 for SIR protein spreading in *Saccharomyces cerevisiae*. Mol Biol Cell 17, 5287–5297.

Zhao K, Chai X, Marmorstein R (2003). Structure of the yeast Hst2 protein deacetylase in ternary complex with 2'-O-acetyl ADP ribose and histone peptide. Structure 11, 1403–1411.